

Frequency modulation of the ion-acoustic instability

H. Klostermann and Th. Pierre*

Equipe Turbulence Plasma, PIIM, UMR 6633 CNRS–Université de Provence, Case 321 Centre de St. Jérôme, F-13397 Marseille Cedex 20, France

(Received 27 October 1999; revised manuscript received 2 February 2000)

In a double-plasma device with a negatively biased grid separating source and target chamber, the ion-acoustic instability is recorded during the injection of an ion beam whose velocity is chosen between the ion-acoustic velocity and twice this value. The observed broad power spectra of the density fluctuations are found to be related to a strong modulation of the frequency inside the bursts of unstable waves. This modulation is interpreted as being a consequence of the existence of propagating strongly nonlinear coherent structures that arise in the course of the nonlinear spatiotemporal evolution of the ion-acoustic instability.

PACS number(s): 52.35.Fp, 52.35.Qz, 52.35.Sb, 52.40.Hf

I. INTRODUCTION

The detailed study of plasma instabilities was an important part of plasma physics research during the two decades 1960–1980. For instance, theoretical and numerical study of the electron-electron two-stream instability has demonstrated the existence of vortices in the phase space [1,2] that are manifested as long-lived coherent spatial structures in configuration space.

The counterpart in the case of ion-ion two-stream instabilities was then investigated by several authors [3–5]. In that case, an ion beam of relative density varying from zero to unity is injected into a stationary plasma. A kinetic description of the system leads to the determination of the instability conditions (positive temporal or spatial growth rate). The dispersion relation depends on four parameters T_e/T_i , T_b/T_i , ω_{pe}/ω_{pi} , and α , where T_e is the electron temperature, T_b the ion beam temperature, T_i the stationary plasma ion temperature, and $\alpha = n_b/n_i$ the relative beam density, i.e., the ratio between the density of the beam n_b and the density of the plasma ions n_i . ω_{pe} and ω_{pi} are the electron and ion plasma angular frequencies.

In typical situations with a moderate beam density, this system is unstable for beam velocities larger than the ion-acoustic velocity c_s in the target plasma, where the Doppler-shifted slow ion-acoustic mode has positive growth rate [6]. The threshold velocity is related to the beam density and temperature [5]. The system is classical in plasma physics laboratory experiments and is known to exhibit turbulent dynamics. A global analysis of the density fluctuations was performed in the early studies, including measurement of the spatiotemporal correlation and of the power spectrum. However, no detailed study of the time series was available at that time.

In this paper, we intend to show that the instability is subject to a considerable frequency modulation and that the spectral broadening observed in previous experiments should not be interpreted as the signature of fully developed turbulence. We show here that the broad power spectrum is in fact

related to the strong spatiotemporal modulation of the beam-plasma system.

The instability under consideration here is of a convective nature. As a consequence, the fluctuations arising in the growth region are amplified by the unstable system. This situation has been studied by Deissler [7] in hydrodynamics in the case of unstable open flow systems. In our situation, this means that the spatiotemporal evolution of the instability in the ion-beam–plasma system on the target side is also closely related to the triggering mechanism in the sheath and presheath region next to the negatively biased grid [8]. It was observed in an earlier numerical study that the evolution of the beam-plasma system strongly depends on the imposed *initial* conditions [9]. Correspondingly, in our experimental system the *boundary* conditions play an important role for the dynamics of the entire system.

The exact origin of the fluctuations inside the sheath of the grid separating the source plasma from the target plasma is not yet fully understood. Space charge oscillations that arise due to the accumulation of ions at the sheath edge are a possible mechanism [8,10,11]. In contrast to thermal noise, these can account for some characteristic scaling properties of the frequency as they are observed.

On the other hand, it is of prime importance to understand the final stage of the instability. It has been shown by several authors [12,13] that, during the spatiotemporal evolution, strong wave-particle interaction leads to the formation of relatively long-lived ion phase-space vortices, the so-called ion holes. In an extended three-dimensional system, continuous growth, interaction, and decay of these structures is believed to govern the turbulent dynamics [14].

Up to now, the main experimental evidence for these coherent structures in unmagnetized laboratory plasmas comes from measurements where conditional averaging has been applied [15]. This technique guarantees a high signal-to-noise ratio due to averaging. However, it does not allow the identification and analysis of single structures in the ion-beam–plasma system, but gives information about the average evolution of the system in a statistical sense. Another drawback is the smearing out that is inherent to averaging techniques.

We report here the results of probe array measurements that give direct access to the spatiotemporal dynamics of the

*Electronic address: tpierre@newsup.univ-mrs.fr

beam-plasma system. Close to the instability threshold, propagating density depressions are observed in accordance with the previous observation of ion holes [14,15]. The existence of these structures accounts for the strong modulation of the frequency inside the bursts of self-excited waves.

II. EXPERIMENTAL SETUP

The double-plasma device consists of a stainless steel vacuum chamber, 35 cm in diameter and 70 cm in length. A grid of 80% transparency with 20 lines per cm separates the source and target chambers, where plasmas can be produced independently by thermionic discharges. Argon is introduced at a pressure $p=2\times 10^{-4}$ mbar. Primary electrons emitted from the heated tungsten filament cathodes are accelerated through a discharge voltage U_d ($U_d=40$ V) toward the respective anodes and ionize neutral argon atoms. The grounded vessel wall represents the target chamber anode whereas the cylindrical source chamber anode is isolated from the latter and can be biased with respect to ground through a bias voltage U_B .

The outer walls of the device are covered with permanent magnets in line-cusp arrangement to confine the primary electrons. The separation grid is biased negatively. The bias voltage U_G exceeds the discharge voltage U_d in absolute value and is chosen typically close to $U_G=-65$ V. This guarantees that all primary electrons are repelled at the space charge sheath that forms around the grid and that only ions can escape from the source chamber.

Plane Langmuir probes of 5 mm diameter are used to determine plasma parameters and to pick up fluctuation signals. The beam is detected by use of a two-grid electrostatic energy analyzer whose energy resolution is 0.2 eV. Moreover, a linear array of eight cylindrical probes of 0.5 mm diameter and 4 mm length each, equally spaced 5 mm from one another, is installed. The array is inclined by an angle of 15° with respect to the axis of the device to reduce shadowing effects.

The plasmas created in both chambers have densities $n=10^8-10^9$ cm $^{-3}$ and electron temperatures $T_e\approx 3$ eV, as determined from plane Langmuir probe characteristics. The ion temperature is inferred from laser-induced fluorescence measurements in a similar device. It is of the order of $T_i\approx 0.1$ eV [16]. Fluctuation signals are recorded with the Langmuir probes biased slightly positively with respect to the plasma potential to detect perturbations in the electron saturation current.

The application of a positive bias U_B to the source anode leads to the injection of an ion beam from the source plasma into the target plasma. The relative beam density is determined by the plasma density in each chamber. After electrostatic acceleration, the ion beam temperature is lower than the plasma ion temperature. However, this beam cooling effect remains small for the moderate beam energies that we consider.

III. EXPERIMENTAL RESULTS

The experiment is conducted with plasmas of comparable densities on either side of the grid. The electrostatic energy analyzer shows relative beam density to be in the range

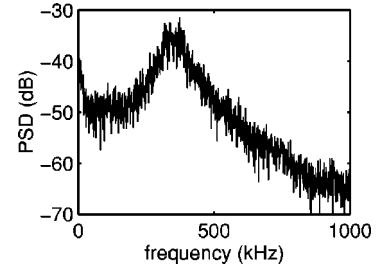


FIG. 1. Typical frequency spectrum of the electron saturation current fluctuations with a plane Langmuir probe when a beam with a velocity slightly above the ion-acoustic velocity is injected. The probe is situated at 3 cm from the grid in the target plasma.

0.1–0.5. In this case, when the bias of the source anode is increased beyond a threshold value, unstable waves propagate as density fluctuations in the target plasma. They are detected as oscillations in the electron saturation current of a Langmuir probe located behind the grid with a phase depending on the probe position. The threshold value of the potential difference $\Delta\phi$ between source and target plasma potentials is approximately $k_B T_e/2$. This corresponds to an acceleration of the injected beam ions to ion-acoustic velocity. The density fluctuations reach a maximum relative fluctuation level of about 10% at a distance of 2 cm from the target side sheath edge and their amplitude decreases with further increasing distance. The power spectrum of the instability is always broad and the frequency of the most unstable mode is about one-half the ion plasma frequency of the target plasma.

Figure 1 shows a typical spectrum of the saturation current fluctuations to a Langmuir probe situated at a few centimeters from the grid on the target side. Although the spectral distribution is very broad, it has a clear maximum at about 400 kHz. Furthermore, we note a contribution at frequencies below 50 kHz. We briefly summarize hereafter some characteristic scaling properties of the instability frequency.

In Fig. 2 is depicted the dependence of the frequency on

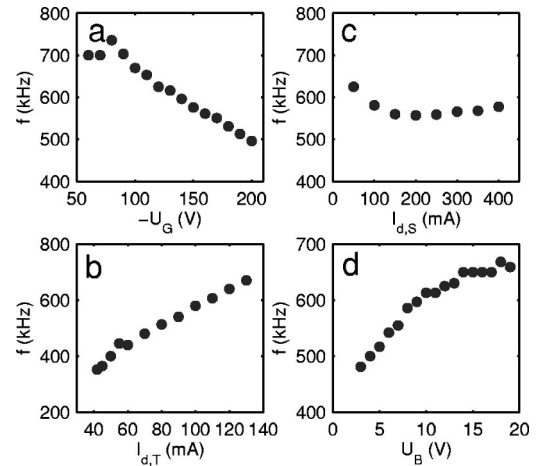


FIG. 2. Dependence of the instability frequency on (a) the grid bias voltage U_G , (b) the target plasma discharge current $I_{d,T}$ which is proportional to the target plasma density n_p , (c) the source plasma discharge current $I_{d,S}$ which is proportional to the beam density n_b , and (d) the bias U_B of the source anode.

different discharge parameters. The frequency decreases with increasing negative grid bias U_G [Fig. 2(a)]. This clearly indicates that the excitation mechanism is related to the ion dynamics in the grid sheath region where the boundary conditions of the ion-beam–plasma system are determined. Indeed, U_G affects the density of ions injected from the grid plane into the sheath in either direction, according to flux conservation. This quantity determines the frequency of space charge oscillations in the grid sheath region as they have been studied in a similar configuration with plasma production restricted to the source chamber [10,11]. The scaling behavior found here is an indication that such processes also play a role in the excitation of the ion-acoustic instability in the ion-beam–plasma system with stationary beam injection.

The frequency of the instability increases with target plasma density [Fig. 2(b)] reflecting a proportionality to the ion plasma frequency of the target plasma. On the other hand, it does not vary much with beam density. The latter is proportional to the source plasma density whose variation has little influence on the frequency [Fig. 2(c)], at least in the range of beam densities compatible with the instability condition. We observe that α must be neither too small nor too large for the instability to appear. Finally, Fig. 2(d) illustrates the increase of the instability frequency with source bias for low values of U_B which turns over into a saturation for higher bias voltages.

The broad power spectra that the system exhibits have formerly been attributed to the existence of a turbulent regime expected under strongly unstable conditions [4]. However, a detailed analysis of the time series using fast sampling digital oscilloscopes reveals that the fluctuating signal is subject not only to amplitude modulation but also to a considerable frequency modulation and it is this fast frequency modulation that leads to the recorded broad power spectra.

Figure 3 shows a time series of the probe signal [Fig. 3(a)] and the results of time-resolved and time-averaged frequency analysis. We find that a significant change of frequency happens within a few oscillation periods so that a short-time Fourier transform does not provide sufficient resolution for the analysis. We therefore take the inverse of the instantaneous oscillation period that is determined from the zero crossings of the bandpass-filtered signal [Fig. 3(b)] as a measure for the fluctuations of the frequency [Fig. 3(c)]. Filtering is necessary, since high- and low-frequency components obscure the evolution of the instantaneous oscillation period of the instability in the main frequency range. The upper and lower cutoff filter frequencies are chosen such that the main peak of the time-averaged spectrum [Fig. 3(d)] lies in the bandpass. They are $f_{low} = 450$ kHz and $f_{up} = 750$ kHz in the case shown.

For consistency, the spectrum in Fig. 3(d) has been calculated from the relatively short time series Fig. 3(a) and therefore has limited spectral resolution. In Fig. 3(b) is shown the low-frequency component of the signal obtained by filtering with a cutoff frequency of 100 kHz.

From Fig. 3(c) one reads that the frequency modulation attains a level of up to 25%, which on average leads to considerable spectral broadening. The values of the inverse instantaneous oscillation period cover the frequency interval

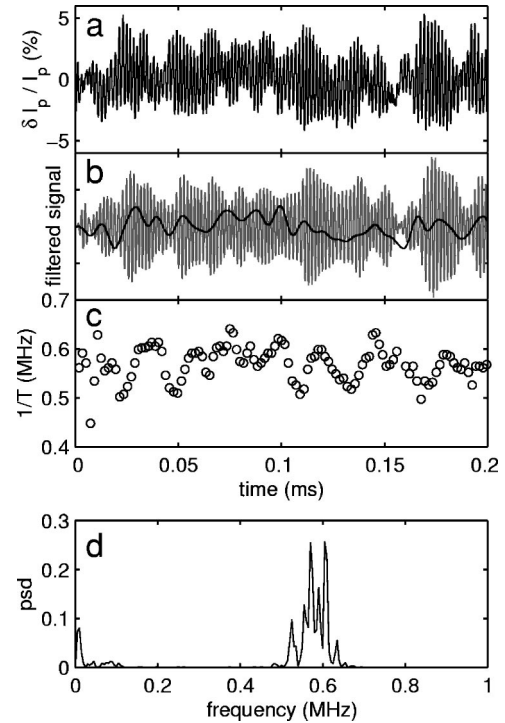


FIG. 3. (a) Time series of the probe electron saturation current signal, (b) the bandpass filtered (400–750 kHz) and low-pass-filtered (100 kHz) signal, (c) the inverse instantaneous oscillation period, and (d) the spectrum of the raw signal for comparison.

with the main spectral contribution to the power spectral density [Fig. 3(d)], as expected.

The temporal evolution of the oscillation period of the bandpass-filtered signal exhibits a strong correlation with the time series of the low-pass-filtered signal. Based on the model for the instability mechanism of the ion-beam–plasma system, we can interpret this finding as follows.

For our experimental parameters ($T_e/T_i \approx 20$, $T_b < T_i$, $\alpha \approx 0.5$, $v_b > c_s$), the system is unstable toward the ion-acoustic instability, i.e., perturbations are growing during the propagation [6]. For beam velocities close to the ion-acoustic speed, the most unstable ion-acoustic mode grows along the beam axis. For beam velocities higher than $2c_s$, the direction of the most unstable ion-acoustic mode is oblique [5]. Since the condition for instability is fulfilled everywhere in the target plasma, the whole volume is unstable as long as the velocity spread of the beam is not too important, so as to restabilize the system.

From previous investigations it is inferred that ion phase-space vortices form in the course of the nonlinear evolution of the instability [9,14,15]. These coherent structures are composed of free-streaming and trapped particles forming a ring-shaped vortexlike structure in phase space. When the physical system under consideration is a counterstreaming beam-plasma system, the ion holes propagate with a velocity close to the ion thermal velocity [18]. On the other hand, when an ion beam is injected into a stationary plasma of the same density, these coherent structures propagate in the laboratory frame at a velocity close to half the beam velocity when the ion beam density equals the density of the ions at rest. In that particular case, the relative beam density is $\alpha = 1$.

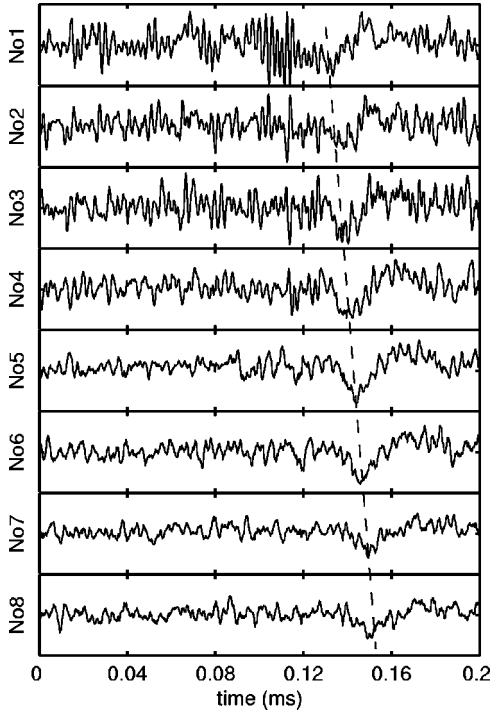


FIG. 4. Simultaneously recorded signals of the eight probes of the probe array. The first probe is at 1 cm from the grid. The distance between probes is 0.5 cm. The density fluctuations are plotted in arbitrary units but the scale is the same for all probes. The dashed line highlights the propagation of the density depression with velocity $v = 2150$ m/s.

In real space, the ion phase-space vortices are manifested as negative potential dips and they are associated with localized plasma density rarefactions. These localized (nonlinear) long-lived coherent structures constitute substantial perturbations of the system parameters. In particular, the local density and velocity of the ion beam fluctuate. At its passage through the dips, the ion beam is accelerated and the density is reduced. It has been shown in earlier work that this strongly affects the spatiotemporal evolution of the system [17]. The observed frequency modulation is one manifestation of the existence of such strongly nonlinear coherent structures.

The evolution of the three-dimensional system in the unstable regime implies the interaction of phase-space vortices that originate from different points in real space. Their continuous growth, interaction, coalescence, and destruction make the identification of single ion holes impossible. To overcome this difficulty, we have chosen a state close to the instability threshold, where it is possible to follow isolated structures. For this purpose, we have performed measurements of the plasma density fluctuations using a probe array. The simultaneous recording of the electron saturation current signals of the probes gives a direct picture of the spatiotemporal evolution of the plasma density. For our experimental parameters and on the relevant time scales of order ω_{pi}^{-1} , the electrons can be assumed to be in local Boltzmann equilibrium. Therefore, the potential perturbation associated with the density rarefaction can be estimated according to $\delta\phi = (k_B T_e / e) (\delta n / n)$.

Figure 4 shows the time series of the eight cylindrical

probes of the array. The first probe is at a distance of 1 cm from the grid, the eighth is at 4.5 cm. The source bias is $U_B = 2$ V, which corresponds to a beam velocity close to the ion acoustic speed. The probe signal has been inverted so that it directly reflects the evolution of the plasma density. At time $t = 0.1$ ms, a burst of unstable waves starts to grow at the grid sheath edge, as can be seen in the time series of probe 1. It reaches large amplitude but its growth is accompanied by a local decrease of the plasma density. This ‘hole digging’ limits further growth, and a strongly nonlinear state is obtained. The emerging density depression proves to be a long-lived structure and can be followed as it propagates along the array (dashed line in Fig. 4). The propagation velocity is $v = 2150$ m/s, which is close to both the ion-acoustic speed and the slow ion beam velocity.

From the temporal duration at a fixed position and the propagation velocity of the density depression we can estimate its size. The full width at half minimum is approximately 2 cm, i.e., of the order of $30\lambda_{De}$.

On the other hand, from its passage through the array a minimum lifetime of $20 \mu\text{s}$ can be deduced, corresponding to 10 oscillation periods. Holes of smaller expansion and shorter lifetime are observed more frequently but the width is not lower than 1 cm. This value agrees with observations of coherent structures in the ion-beam–plasma system by other authors [9,15,17]. However, it is greater than the predicted width of ion holes in the case of counterstreaming ion populations [18]. For a deeper understanding of this discrepancy, a theoretical study of the stability of coherent structures in the case of the ion-beam–plasma system is needed.

IV. DISCUSSION AND CONCLUSION

We have reported here the existence of a large frequency modulation of the unstable wave packets of the ion-acoustic instability observed in an ion-beam–plasma system. This frequency modulation leads to broad power spectra, as have been observed by several authors. To the best of our knowledge, we have also reported the first direct observation of propagating coherent structures in nonaveraged time series in the ion-beam–plasma system.

Comparing our findings to earlier experimental and numerical studies [14,15,17,19], we have identified the observed structures as ion phase-space vortices, which in real space are manifested as density depressions and associated negative potential dips. They result from strong wave-particle interaction in the course of the nonlinear evolution of the ion-acoustic instability. The width of these structures, their propagation velocity, and the order of their lifetime are consistent with previous findings in a similar system, where conditional averaging was applied [15]. These investigations were supported by numerical simulations [14]. Similar structures have been observed in ion beam–plasma systems with application of a steplike perturbation to the beam velocity [17,19]. In these previous studies, as well as in our investigations, the coherent structures are found to have widths of the order of $(20-30)\lambda_{De}$ and to propagate with a velocity of the order of the slow beam velocity.

Schamel and co-workers have derived analytically localized solutions of the one-dimensional Vlasov-Poisson system to describe such ion holes in a plasma with counterstreaming

ion populations. In that case, the holes move with a velocity of the order of the ion thermal velocity and their width is typically a few electron Debye lengths [12,18]. However, numerical and experimental investigations show that in experiments with ion beam injection into a plasma at rest, holes of larger extent can develop and that these propagate with a velocity that is rather of the order of the ion-acoustic velocity than of the ion thermal velocity in the laboratory frame of reference.

To identify isolated coherent structures, we have chosen a state close to the instability threshold for the probe array measurements. In this case, it can be expected that structures forming at a certain location in space can evolve free from competition with neighboring ones.

In the fully unstable three-dimensional system, interaction of competing ion phase-space vortices that originate from different locations prohibits the identification of single holes. Nevertheless, they constitute a low-frequency component in the fluctuation signals that propagates at the slow ion beam velocity, which is typically close to the ion-acoustic velocity in the case of unstable waves.

In summary, our investigations help to clarify the evolution of the double-plasma–ion-beam system under unstable

conditions. They show that the existing fluctuations inside the grid sheath play an important role in the excitation of unstable ion-acoustic waves that propagate in the ion-beam–plasma system on the target side. Time-resolved frequency analysis reveals that the broad frequency spectra of the unstable waves are due to frequency modulation that is related to the local modulation of the ion-beam–plasma system inside the bursts. This nonlinear behavior is ascribed to the interaction with ion phase-space vortices that originate from the strong wave-particle interaction in this unstable system.

In addition, spatiotemporal probe array measurements have allowed direct observation of these structures in the form of propagating density depressions. These investigations present experimental confirmation of the current model describing the wave-particle interaction in the unstable ion-beam–plasma system.

ACKNOWLEDGMENTS

One of the authors (H.K.) gratefully acknowledges support from the Alexander von Humboldt Foundation (Germany). We thank Dr. G. Leclert for a critical reading of the manuscript.

-
- [1] K. V. Roberts and H. L. Berk, *Phys. Rev. Lett.* **19**, 297 (1967).
 - [2] M. Kako, T. Taniuti, and T. Watanabe, *J. Phys. Soc. Jpn.* **31**, 1820 (1971).
 - [3] R. J. Taylor and F. V. Coroniti, *Phys. Rev. Lett.* **29**, 34 (1972).
 - [4] Y. Kiwamoto, *J. Phys. Soc. Jpn.* **37**, 466 (1974).
 - [5] F. Doveil and D. Grésillon, *Phys. Fluids* **18**, 1756 (1975).
 - [6] B. D. Fried and A. Y. Wong, *Phys. Fluids* **9**, 1084 (1966).
 - [7] R. J. Deissler, *J. Stat. Phys.* **54**, 1459 (1989).
 - [8] A. Sarma, H. Bailung, and J. Chutia, *Phys. Plasmas* **3**, 3245 (1996).
 - [9] H. L. Pécseli, J. Trulsen, and R. Armstrong, *Phys. Scr.* **29**, 241 (1984).
 - [10] H. Klostermann, A. Rohde, and A. Piel, *Phys. Plasmas* **4**, 2406 (1997).
 - [11] A. Rohde, H. Klostermann, and A. Piel, *IEEE Trans. Plasma Sci.* **25**, 1144 (1997).
 - [12] S. Bujarbarua and H. Schamel, *J. Plasma Phys.* **25**, 515 (1981).
 - [13] H. L. Pécseli and J. Trulsen, *Phys. Rev. Lett.* **48**, 1355 (1982).
 - [14] H. L. Pécseli and J. Trulsen, *Phys. Fluids B* **1**, 1616 (1989).
 - [15] H. Johnsen, H. L. Pécseli, and J. Trulsen, *Phys. Fluids* **30**, 2239 (1987).
 - [16] G. Bachet, L. Chérigier, M. Carrère and F. Doveil, *Phys. Fluids B* **5**, 3097 (1993).
 - [17] G. Bonhomme, Th. Pierre, G. Leclert, and J. Trulsen, *Plasma Phys. Controlled Fusion* **33**, 507 (1991).
 - [18] H. Schamel, *Phys. Rep.* **140**, 161 (1986).
 - [19] P. H. Sakanaka, *Phys. Fluids* **15**, 1323 (1972).